Cell, Vol. 85, 745–759, May 31, 1996, Copyright ©1996 by Cell Press

Perturbation of Nuclear Architecture by Long-Distance Chromosome Interactions

Abby F. Dernburg,*§ Karl W. Broman,† Jennifer C. Fung,‡ Wallace F. Marshall,* Jennifer Philips,* David A. Agard* and John W. Sedat*
*Department of Biochemistry and Biophysics
University of California, San Francisco
San Francisco, California 94143-0554
†Department of Statistics
University of California, Berkeley
Berkeley, California 94720
‡Graduate Group in Biophysics
University of California, San Francisco
San Francisco, California 94143-0554

Summary

Position–effect variegation (PEV) describes the stochastic transcriptional silencing of a gene positioned adjacent to heterochromatin. Using FISH, we have tested whether variegated expression of the eye-color gene *brown* in Drosophila is influenced by its nuclear localization. In embryonic nuclei, a heterochromatic insertion at the *brown* locus is always spatially isolated from other heterochromatin. However, during larval development this insertion physically associates with other heterochromatic regions on the same chromosome in a stochastic manner. These observations indicate that the *brown* gene is silenced by specific contact with centromeric heterochromatin. Moreover, they provide direct evidence for long-range chromosome interactions and their impact on three-dimensional nuclear architecture, while providing a cohesive explanation for the phenomenon of PEV.

Introduction

Models for the regulation of genetic activity by the global arrangement of chromosomes in interphase nuclei have proliferated in recent literature (cf. Manuelidis, 1990; Cremer et al., 1993; Palladino and Gasser, 1994). Testing such models has proved challenging because of the difficulty of observing decondensed chromosomes during the crucial stage at which transcription occurs. However, the development of chromosome in situ hybridization methods, particularly fluorescence in situ hybridization (FISH), has made it possible to localize particular portions of the genome within intact nuclei, even during interphase. Here we have combined FISH with three-dimensional microscopy and statistical analysis to test a structural model for position–effect variegation (PEV) in Drosophila.

PEV (reviewed by Spofford, 1976; Weiler and Wakimoto, 1995) is an epigenetic phenomenon associated with heterochromatic regions of the genome. When a gene is moved to a position near a block of centromeric heterochromatin by chromosome rearrangement, its transcription will often be affected in a curious manner: the gene is expressed in some cells but is silent in others, resulting in a mosaic pattern that can be readily detected if the gene affects, for example, tissue pigmentation. The prevailing model for this phenomenon invokes a "spreading" mechanism, in which the condensed transcriptionally silent state of heterochromatin extends along the length of the chromosome into neighboring genes. The extent of this spreading is proposed to vary on a cell-by-cell basis, accounting for the variegated phenotype.

However, there are particular examples of PEV that do not appear to mesh with this general model. The most deviant example is probably the dominant PEV induced by certain alleles of the *brown* (*bw*) gene. The $brown^{Dominant}$ (bw^D) allele is a null mutation caused by an insertion of a large block of heterochromatin into the coding sequence of the gene (Slatis, 1955), which lies near the end of the right arm of chromosome 2 (Figure 1). It has the unique property of being able to cause variegated inactivation of a normal copy of the gene present on a homologous chromosome. The genetic dominance is dependent on physical pairing between the bw^D chromosome and its wild-type homolog (Dreesen et al., 1991), analogous to a number of other known genetic phenomena (Tartof and Henikoff, 1991).

A model has been proposed by Henikoff (1994, 1996) to explain the "*trans*-inactivation" caused by bw^D. According to this view, the insertion of heterochromatin into one copy of *bw* (the bw^D allele) causes it to move to a heterochromatic compartment of the nucleus. When this mutant allele is paired with a wild-type copy of the gene, it drags the intact gene along with it to an abnormal nuclear position. In this new environment, the transcriptional activity of the wild-type allele is repressed. The primary evidence leading to this model is that the strength of *trans*-repression by the bw^D allele is strongly influenced by its chromosomal position. Its effect can be suppressed by chromosome rearrangements that move the region containing bw^D to a position more distant from centric heterochromatin (Talbert et al., 1994). Conversely, translocation of bw^D to a more centromere-proximal position strengthens its silencing ability (Henikoff et al., 1995). The crux of this hypothesis is that the bw^D allele inactivates transcription through physical association with centromeric heterochromatin. This is a provocative model in that it postulates at least three ideas for which direct evidence is currently scant or lacking: that the position of a gene within the nucleus can be influenced by neighboring sequences, that this change in localization can affect a homologous copy of the gene in *trans*, and that the resulting mislocalization can, in turn, lead to altered expression.

Here, we test this model for regulation of gene expression in diploid nuclei. Using FISH, we hybridized interphase nuclei with probes to the *bw* locus and to specific blocks of heterochromatin. We show that the organization of chromosome 2 is dramatically altered by insertion of heterochromatin at a distal position: whereas normally the *bw* locus shows no tendency to

§Present Address: Department of Developmental Biology, B300 Beckman Center, Stanford University, Stanford, California 94305.

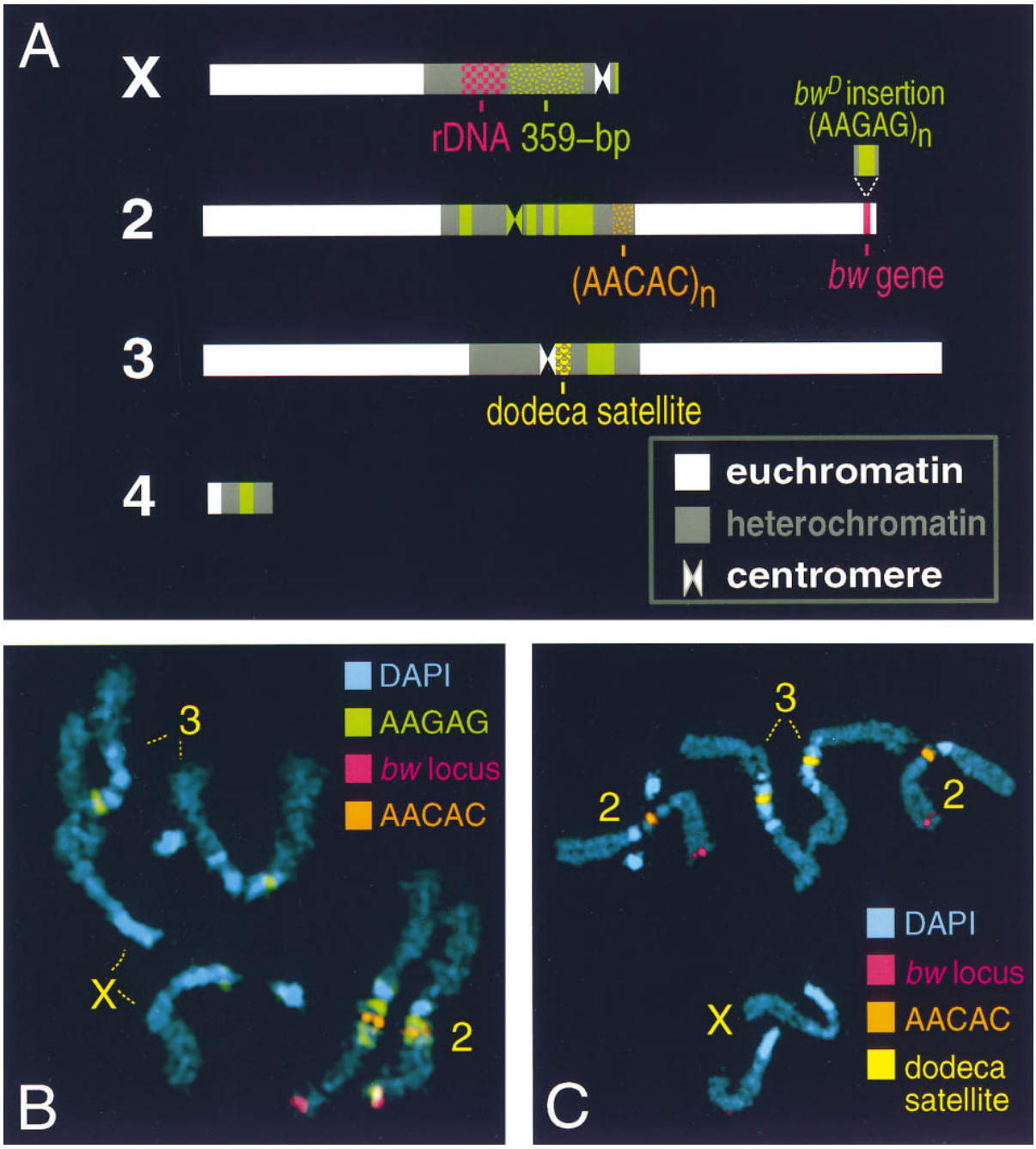

Figure 1. Genomic Positions of the Loci Examined in This Study

(A) Diagram of the four Drosophila chromosomes (our experiments are restricted to female nuclei, so the Y chromosome is not shown). The chromosome-specific loci are labeled, and the distribution of the AAGAG satellite, which is present on all four chromosomes, is marked by solid green boxes (adapted from Lohe et al., 1993). The colors used for each locus are consistent throughout the subsequent figures.

(B) and (C) Mitotic chromosomes from heterozygous bw^D female larvae ($bw^D/+$). In (B), the bw^D insertion, which hybridizes with the AAGAG satellite probe, is detected at the *bw* locus on one of two copies of chromosome 2.

associate with centromeric heterochromatin, in bw^D nuclei this distal locus frequently pairs with the centromeric region of its own chromosome. Moreover, as predicted by the model, in heterozygotes ($bw^D/+$) the bw^D allele pairs with the wild-type allele and causes it to associate with centromeric heterochromatin. We demonstrate that this phenomenon is due to specific intrachromosomal associations, probably based on homology, and not simply to a tendency of heterochromatin to occupy a particular region of the nucleus. Furthermore, this change in nuclear architecture demonstrates a marked developmental progression: in early embryonic

development, such associations are never detected, but in two different larval tissues, association is observed in 25%–86% of nuclei.

We also show that this strong tendency of chromosomes to form ectopic homologous associations is not restricted to the bw^D insertion nor to the particular satellite sequence it contains, but instead probably reflects a general property of heterochromatic sequences. Our results are consistent with a model in which such interactions over large genomic distances are a consequence of chance interactions between different chromosome regions, the likelihood of which increases with the duration of interphase.

Results

Telophase Polarity Is Maintained during Interphase in Blastoderm Embryos and Is Unaffected by the bw^D Mutation

As described above, the dominant variegation caused by the bw^D mutation results from insertion of a block of heterochromatin into one copy of the *bw* gene. This insertion is estimated to exceed 2 Mb in size and has been shown to hybridize with chromosome probes containing the sequence $(AAGAG)_n$ (P. Dimitri and S. Pimpinelli, personal communication; Figure 1). In Drosophila, the chromosome regions flanking the centromeres contain many megabases of such tandemly repeated "satellite" sequences, which are not normally found elsewhere along the arms. This particular AAGAG repeat associated with the bw^D insertion is one of the most abundant in the genome. It is detectable on each of the Drosophila chromosomes and is particularly well represented in the pericentric region on chromosome 2, the same chromosome that carries the *bw* gene (Lohe et al., 1993). In Figure 1, the genomic positions of the *bw* gene and the satellite sequences described in this study are shown.

We first investigated the effect of this mutation on nuclear organization in Drosophila embryos. During the 14 nuclear divisions preceding gastrulation, most of the nuclei lie in a single layer near the outer membrane of the embryo, and they all show the same polarity with respect to that surface: centromeres are found in the apical region of the nuclei, nearest the surface, and telomeres tend to reside in the inner, or basal, portion of the nuclei (Figure 2A). This polarity is evident by direct reconstruction of nuclei stained with DAPI at prophase (Hiraoka et al., 1990a), and during interphase it can also be observed using FISH (Marshall et al., 1996). The *bw* gene maps to cytological region 59E, near the end of the right arm of chromosome 2 (2R) (Lindsley and Zimm, 1992; see Figure 1), and might thus be expected to localize to a basal nuclear position.

We examined the nuclear position of *bw* using a fluorescent probe to the coding sequence of the gene (see Experimental Procedures). In wild-type embryos, both copies of the gene localized basally in every nucleus (Figures 2B and 2C). The two homologous copies of the gene did not colocalize at this stage, consistent with observations that pairing between homologous chromosomes only begins near the end of the syncytial blastoderm stage of development (Hiraoka et al., 1993).

There was no significant difference in the vertical position of the *bw* loci in the nuclei of embryos carrying either one or two copies of the bw^D chromosome, compared with wild-type (Figure 3; see Figure 2). To observe the positions of the *bw* loci relative to the bulk of heterochromatin, we hybridized embryos with both a *bw* gene probe and a probe to the AAGAG satellite. The fluorescent signals from centromeric blocks of this satellite sequence were restricted to the apical portion of the nucleus. An additional signal from the satellite probe was observed in close proximity to the position of the *bw* probe in bw^D but not in wild-type embryos (see Figures 2B–2E). That insertion of this sequence at a distal position (into the *bw* gene) causes it to localize to an atypical position within the nucleus suggests that a primary determinant of the localization of the AAGAG satellite in embryonic nuclei is its position along the length of a chromosome arm.

To see whether the *bw* locus associates with other heterochromatin, we determined the nuclear position of a second satellite sequence, $(AACAC)_n$. This satellite is restricted to a single region in the pericentric heterochromatin on 2R (Makunin et al., 1995; see Figure 1B). Like the pericentric blocks of the AAGAG satellite, it localizes apically in blastoderm nuclei and never comes into contact with the *bw* gene (Figure 3). Moreover, when the positions of other blocks of satellite sequence in embryonic nuclei were determined, all except for a *Y* chromosome repeat were restricted to the apical portion of the nucleus (Marshall et al., 1996). Hence, in blastoderm stage embryos, the *bw* gene is physically isolated from centromeric heterochromatin.

Insertion of satellite DNA into the *bw* gene did not affect the degree of association between homologous chromosomes at that locus. In both wild-type and homozygous bw^D embryos, no pairing of *bw* loci was detected in nuclear cycle 13, but in interphase 14 the locus was between 50%–70% paired, comparable to other loci we have examined (J. C. F., A. F. D., W. F. M., and J. W. S., unpublished data).

Although the bw^D insertion did not affect pairing or vertical placement of the locus, the insertion of a block of heterochromatin appeared to target the *bw* locus to the nuclear envelope (Figure 3). Whereas normally the gene is located at random with respect to the envelope, in bw^D embryos both copies of the locus are nonrandomly close to the nuclear periphery when evaluated statistically, as described by Marshall et al. (1996). This intriguing observation is discussed below.

Nuclear Architecture Is Different in Embryonic and Larval Tissues

Since the variegation caused by bw^D affects adult eye color, the mutation is most likely to affect expression in the eye imaginal disks during larval or pupal development. (Dreesen et al., 1988). We therefore examined the behavior of the locus in larval eye disks, a tissue more likely than embryos to be expressing *bw*. Since the pairing of homologous chromosomes is not completed by the end of the embryonic blastoderm stage (Hiraoka et

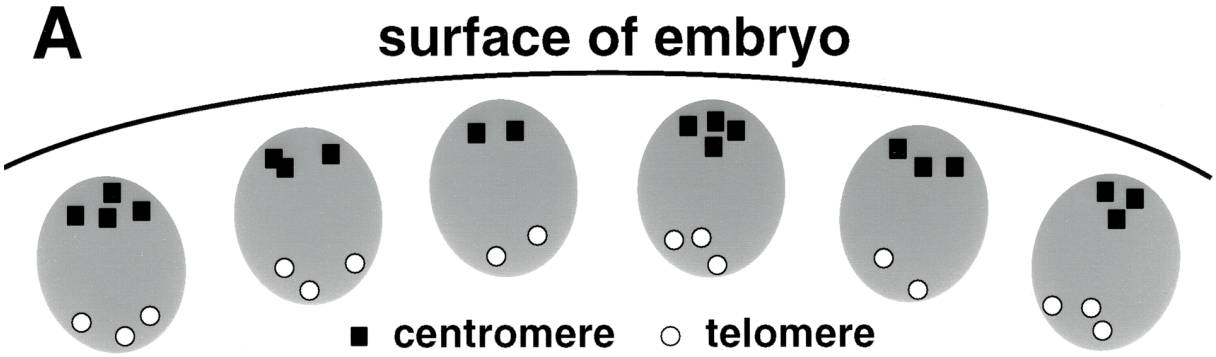

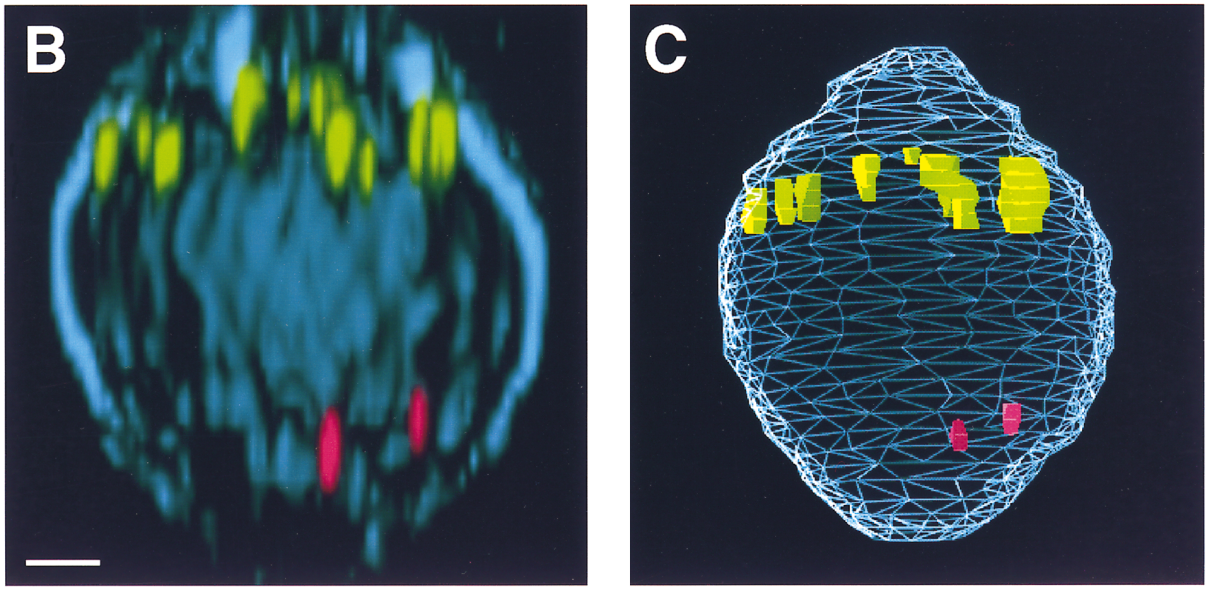

nucleus from a wild–type embryo

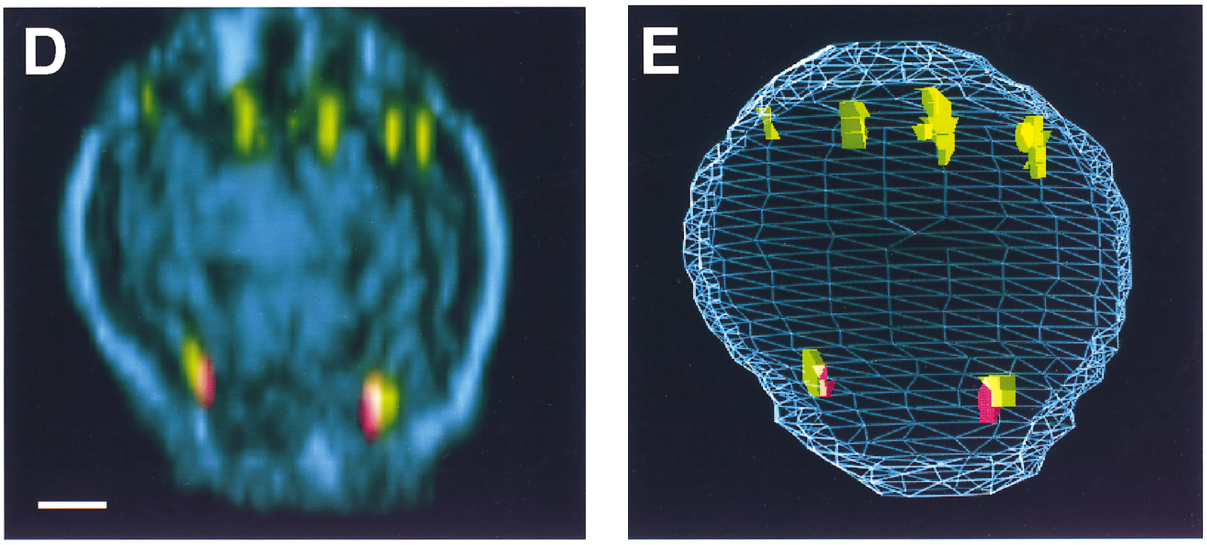

nucleus from a bw^D/bw^D embryo

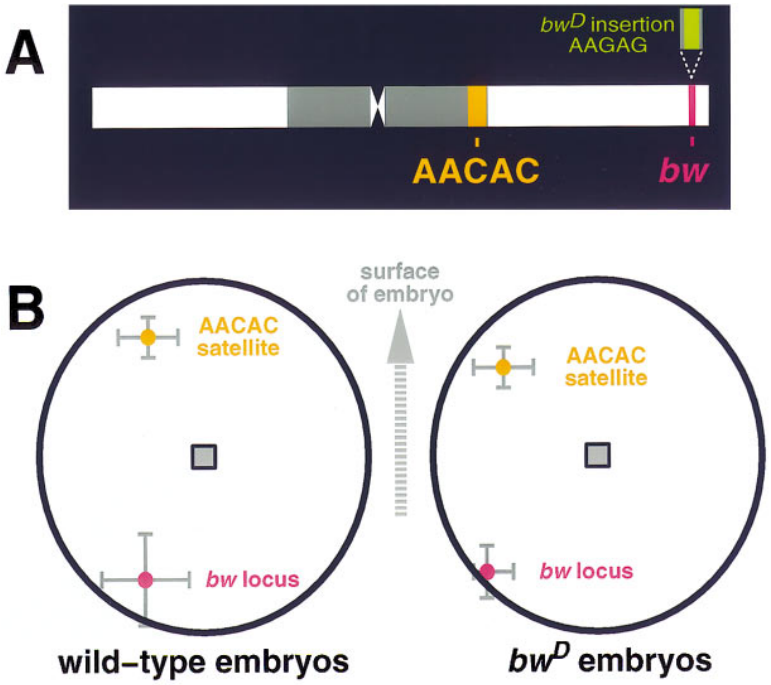

C

vertical distance from center of mass (μm)

	wild–type	bw^D
AACAC	2.05 +/– 0.46 (n=105)	1.40 +/– 0.35 (n=140)
bw locus	–2.16 +/– 0.77 (n=77)	–2.00 +/– 0.46 (n=81)

distance from nuclear envelope (μm)

	wild–type	bw^D
AACAC	1.15 +/– 0.46 (n=105)	0.92 +/– 0.46 (n=140)
bw locus	0.67 +/– 0.67 (n=77)	0.13 +/– 0.34 (n=81)

Figure 3. Diagram of the Positions of the *bw* Locus and the AACAC Satellite in Nuclei from Wild-Type and bw^D Embryos

Numerical values are given below; all distances are measured in microns. The grey square in each nucleus represents the center of mass, and the position along the vertical (apical–basal) axis for each locus is measured from this point. The AACAC satellite is constrained to lie in the apical region of embryonic nuclei, while the *bw* locus is restricted to a basal location. These two loci are thus never in contact. The horizontal axis represents the distance of each locus from the nuclear envelope, marked with an anti-lamin antibody. In wild-type embryos (left), both AACAC and *bw* localize at random with respect to the nuclear envelope, but in bw^D embryos (right) the heterochromatic insertion at the *bw* locus results in nonrandom association of the gene with the nuclear periphery. All measurements and analysis were performed as described by Marshall et al. (1996).

al., 1993), it was conceivable that aspects of nuclear architecture affecting genes expressed later in development might not be manifested in the embryo.

In imaginal disks from female larvae carrying bw^D, the chromosome arrangement observed with different probe combinations was markedly different from that seen in embryos. Heterochromatic probes were often far apart from each other, as opposed to the clustered arrangement typical of embryonic nuclei. Furthermore, homologous bw^D loci were almost always paired and were frequently observed in close proximity to the AA CAC satellite on 2R (Figure 4), whereas in embryonic nuclei the AACAC satellite was consistently distant from the *bw* locus (see Figure 3). These differences emphasize the importance of studying nuclear architecture within a developmental context.

Figure 2. Localization of Satellite DNA and the *bw* Gene Locus in Embryonic Nuclei

(A) Schematic cross-section through nuclei in a Drosophila blastoderm embryo. Telophase polarity of the nuclei is maintained throughout interphase, as evidenced by observations that centromeric probes tend to localize apically (close to the surface of the embryo) and telomeric probes basally in each nucleus.

(B) Volume-rendered projection, and (C) wire-frame model of a nucleus from a wild-type embryo, hybridized with an 8.4 kb probe to the *bw* gene (magenta) and an oligonucleotide probe to the AAGAG satellite (green). The apical portion of the nucleus is towards the top of each image. The AAGAG satellite, which is normally restricted to the centromeric heterochromatin (Figure 1), shows multiple apical signals in the nucleus, while the distally located *bw* gene is near the opposite basal side. Two signals are seen for the *bw* probe, indicating that the homologous copies of chromosome 2 are not paired at this locus.

(D) and (E) A nucleus from a homozygous bw^D embryo, hybridized with the same two probes. The distribution of the AAGAG satellite is similar to that seen in wild-type embryos, except that a new fluorescent signal is detected near each of those from the *bw* locus probe. Scale bars in (B) and (D), 1 μm.

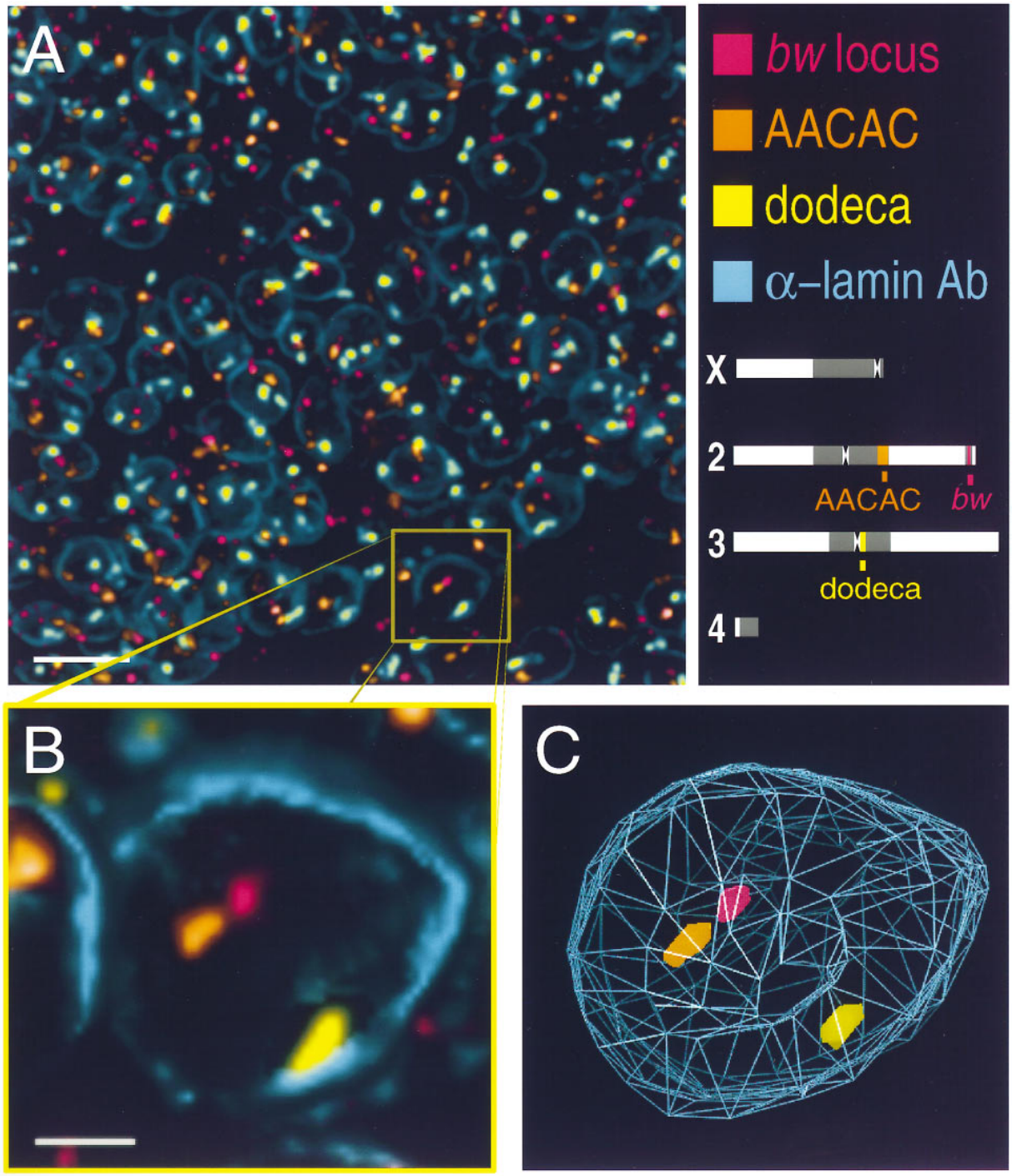

Figure 4. Association between the *bw* Gene and Heterochromatin in Imaginal Disk Nuclei

(A) Projection through a 2 μm optical slice of a whole-mount eye disk from a female third instar larva. The top right panel indicates the probes employed in this experiment and their map positions. Scale bar, 5 μm.

(B) and (C) In some nuclei, such as the one in the yellow box in (A), the *bw* gene can be seen in proximity to the AACAC satellite (orange), although these loci are far apart on the chromosome arm and are never seen in proximity in embryonic nuclei. Scale bar in (B), 1 μm. (C) is a wire-frame model of the nucleus shown as a volume-rendered projection in (B).

bw^{D} Associates with a Centromeric Satellite Sequence in Diploid Drosophila Larval Tissues

Since our initial observations in eye imaginal disks revealed a complex relationship between *bw*^{D} and the AACAC satellite, we analyzed their spatial relationship in more detail. Because imaginal disk cells are very small and densely packed, we could only characterize the distribution of fluorescent probes in a tiny fraction of

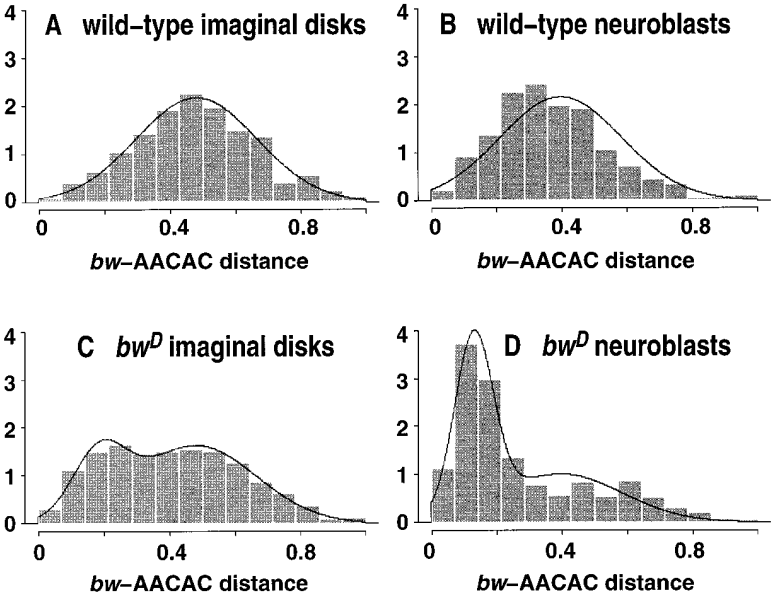

Figure 5. Histograms of the Normalized Distances between the *bw* Gene and the AACAC Satellite for Wild-Type and bw^D Nuclei, from Both Eye/Antennal Disks and Neuroblasts

The curves correspond to the fitted distributions; for the wild-type nuclei, this is a truncated normal distribution, whereas for the bw^D nuclei, it is a mixture of two truncated normal distributions, with one component constrained to be equal to the corresponding wild-type distribution (see Results and Experimental Procedures for details).

nuclei in whole-mount preparations. To obtain more quantifiable data, we analyzed the distribution of the two loci in nuclei from larval brain squash preparations. We performed similar experiments on squash preparations of eye/antennal imaginal disks to compare chromosome organization between these two diploid tissues (see Experimental Procedures).

We measured the distance between the *bw* locus and different chromosome-specific satellite blocks. To correct for differences in preparation between samples, the distance measurements were normalized by expressing them as a fraction of the nuclear diameter, as described in Experimental Procedures. These distances were plotted as histograms (Figure 5). A striking and consistent difference was immediately apparent between wild-type and bw^D nuclei in the distribution of distances between *bw* and the AACAC satellite block on 2R . These distances could be accurately modeled in wild-type nuclei by a normal distribution, truncated at 0 and 1 (Figures 5A and 5B). This suggests that the two loci are randomly located with respect to each other, with a slight skew toward shorter distances observed in neuroblast nuclei. However, in bw^D nuclei, there appeared to be two overlapping distributions of distances, one similar or identical to the wild-type pattern, and a new distribution centered at a much shorter distance (Figures 5C and 5D). The simplest interpretation of this result is that the *bw* gene is unusually close to the AACAC satellite in a subset of nuclei, but in other nuclei it remains randomly positioned with respect to AACAC. To evaluate whether the data were consistent with this idea, we modeled the distribution of the measured *bw*–AACAC distances as a mixture of the observed wild-type distribution and a second normal distribution. To analyze the mixture rigorously, we used a maximum likelihood estimation method (Titterington et al., 1985). A detailed description of the model used for this analysis is given in Experimental Procedures.

Using this statistical approach, we found that the distances between bw^D and the AACAC satellite were very reasonably approximated by a mixture of two normal distributions. Given the degree of fit between the model and the data, the fraction of nuclei contributing to each peak within the mixture could be estimated with an estimated SD of 3%. As summarized in Table 1, we estimate that bw^D is associated with the AACAC pericentromeric heterochromatin in 25%–86% of diploid larval nuclei, depending on both the tissue and the developmental stage.

We defined the peak of shorter distances in nuclei carrying bw^D as "nuclei exhibiting association." Because the distances within this distribution are nonzero, it is very improbable that the bw^D insertion is associating directly with the AACAC satellite. Instead, it is likely to contact a nearby region in the centric heterochromatin. The variation in distance from *bw* to AACAC within this distribution could reflect association of bw^D with a number of different sites at varying distances from the AACAC block, or association with one site whose distance from AACAC varies due to fluctuations in chromosome conformation, or a combination of these effects.

These results suggested that the bw^D insertion, which contains the AAGAG repeat, might be associating with other blocks of this same sequence in the heterochromatin near the block of AACAC repeats on chromosome 2 (see Figures 1A and 1B). We attempted to test this directly by hybridizing larval nuclei with AAGAG probes, but this was unsuccessful because the distribution of this abundant satellite was highly dispersed in such nuclei, and the fluorescent signals corresponding to chromosome 2 heterochromatin and the bw^D insertion could not be identified. However, this provides evidence that all heterochromatin does not occupy a single small territory in interphase nuclei.

Insertion of Satellite DNA at One *bw* Locus Causes Both Gene Copies to Associate with Heterochromatin

The two homologous copies of the *bw* locus are paired in greater than 95% of larval nuclei. This is typical of

Table 1. Estimated Association Frequencies Between the *bw* Locus and the AACAC Satellite

					Proportion of Nuclei Exhibiting Association				
					Third Instar Larvae at Room Temperature		bw^D/bw^D		
Tissue	m1	s1	m2	s2	bw^D/bw^D	$bw^{D}/+$	16°C	Second Instar	Prepupae
Neuroblast nuclei									
Estimate	0.41	0.20	0.14	0.07	0.57	0.54	0.61	0.86	0.69
(Estimated SD)	(0.01)	(0.01)	(0.01)	(0.01)	(0.03)	(0.03)	(0.03)	(0.03)	(0.03)
Eye/antennal imaginal disks									
Estimate	0.48	0.19	0.19	0.08	0.25				
(Estimated SD)	(0.01)	(0.01)	(0.01)	(0.01)	(0.03)				

A value is given for the mean and SD of each normal distribution contributing to the mixture.
Abbreviations: m, mean; s, SD. (Estimated SD) refers to the SD of each estimated value.

loci we have examined from other regions of the genome. The pairing frequency is unchanged when wild-type, $bw^D/+$, and bw^D/bw^Dnuclei are compared. We measured the distance between the single fluorescent signal from the *bw* locus probe and the AACAC probe in both homozygous (bw^D/bw^D) and heterozygous ($bw^D/+$) neuroblast nuclei (Table 1). Surprisingly, the frequency of association of paired *bw* loci with the AACAC satellite was only slightly lower when only one of two copies of chromosome 2 carried the bw^D insertion. Thus, a single copy of the insertion can mediate association with heterochromatin nearly as well as two copies and can carry a wild-type copy with it as a consequence of pairing between homologous chromosomes.

The data presented in Table 1 demonstrate that nuclear organization differs between neuroblasts and eye disks, which is also evident from the histograms presented in Figure 5. Eye disks show a markedly lower degree of association between bw^D and AACAC: only 25% of nuclei exhibit this association, compared with nearly 60% of neuroblast nuclei from the same stage of development. In neuroblasts, we detected a greater degree of association in both second instar and pupariated larvae than during the climbing third instar period. The differences observed between the different tissues and varying stages within the same tissue could be due to developmentally regulated expression of particular gene products, or to the rate at which nuclei are undergoing mitotic division (discussed below).

bw^D Associates with Specific Centromeric Heterochromatin Sequences

To determine whether bw^D associates with specific heterochromatic sequences or simply has a general affinity for heterochromatin, we measured the position of the *bw* gene in wild-type and bw^D nuclei in relation to chromosome-specific satellites from the two other major chromosomes: the 359-bp satellite on the X chromosome (Hsieh and Brutlag, 1979; Lohe et al., 1993; see Figure 7A) and the dodeca satellite near the centromere of chromosome 3 (Abad et al., 1992; Carmena et al., 1993; see Figure 1B). We analyzed neuroblasts and eye/antennal disks from female larvae. Only the distance between *bw* and the chromosome 2–specific satellite showed a marked change between wild-type and bw^D nuclei (Figure 6).

This demonstration that association of the gene with AACAC is specific deviates from the model being tested, which proposes a general affinity of heterochromatin for other heterochromatin. Instead, the effect of the bw^D insertion is a specific association of the *bw* gene with other heterochromatin on chromosome 2. Moreover, our measurements show that the *bw* gene can simultaneously be near to AACAC and far from heterochromatin on other chromosomes (see the scatter plots in Figure 6). This further supports the conclusion that heterochromatin is dispersed in the interphase nucleus.

Other Distal Heterochromatin Behaves in a Manner Analogous to the bw^D Insertion

We wished to test whether the association of distally translocated heterochromatin with centric heterochromatin is unique to the bw^D insertion, or instead represents a more general phenomenon. To do so, we asked whether distal heterochromatin on an inverted X chromosome can pair with a homologous region located near the centromere on a partner chromosome. We examined nuclei heterozygous for a normal X chromosome and FM7, a rearranged X that carries a large block of heterochromatin at its distal end (Lindsley and Zimm, 1992; Figure 7).

Analogous to observations of the bw^D chromosome, in embryos the vertical localization of X heterochromatin was largely or solely determined by its position along the length of the X chromosome (Figures 7D–7F). In wild-type embryos, the X heterochromatin was restricted to the apical region of each nucleus, but when FM7 was present, its distal heterochromatin was detected at a basal position. By interphase of nuclear cycle 14, normal X chromosomes are frequently paired in their heterochromatic regions, but pairing between X and FM7 was never observed (Figures 7C–7F).

In imaginal disk and neuroblast nuclei, however, the large blocks of heterochromatin on X and FM7 were often paired, indicating that the centromeric region of the X chromosome interacts with the telomere of FM7. We measured the frequency of this interaction in neuroblast squashes and found that the heterochromatin on the normal X was paired with that on the inverted chromosome in 75% of nuclei from larvae raised at room temperature (20°C–22°C; n = 444 nuclei from three animals). This value dropped to 42% if the larvae were

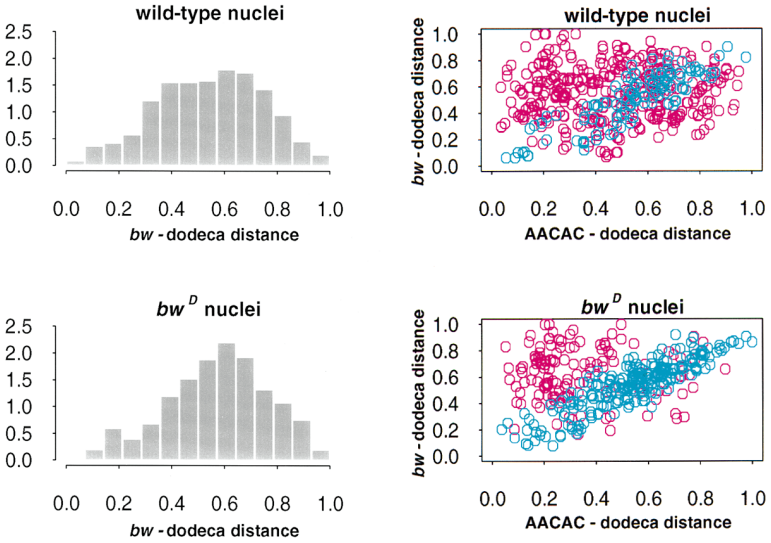

Figure 6. Specificity of the Association between the *bw* Locus and the AACAC Satellite

The plots on the left display histograms of the normalized distances between the *bw* locus and the dodeca satellite on chromosome 3 (see Figure 1 for the map positions of these loci). Data from wild-type and bw^D third instar neuroblasts are given. There is a subtle difference between the two genotypes, but far less dramatic than that seen in Figure 5. The two scatter plots demonstrate that this is an indirect consequence of specific association between the *bw* locus and heterochromatin on chromosome 2. In these plots, each point represents a normalized *bw*–dodeca distance plotted against the normalized AACAC–dodeca distance for the same nucleus. Nuclei in which the *bw* locus is within 25% of the nuclear diameter of the AACAC satellite are indicated in blue, and those with greater *bw*–AACAC separation are magenta. Among those (magenta) nuclei in which *bw* is not close to AACAC, there is no increased tendency for it to associate with the dodeca satellite in bw^D nuclei compared to wild-type. This is also true if only those (blue) nuclei in which the *bw* locus is close to the AACAC satellite are considered. Thus, the relationship between the *bw* locus and the dodeca satellite is unaffected by the bw^D mutation. The difference between the *bw*–dodeca distribution in the two genotypes is attributable to the fact that in bw^D nuclei, there are far more nuclei in which *bw* is close to AACAC than in wild-type. Similar results were obtained using Q–Q plots (data not shown).

raised at 16°C (n = 439 nuclei from five animals). This contrasts with the association of bw^D with centric heterochromatin, the frequency of which shows no statistically significant difference over this range of temperatures (Table 1). Nevertheless, these observations demonstrate that heterochromatin in larval nuclei participates in physical interactions that violate the polarized organization of embryonic nuclei, mirroring our results with bw^D.

Discussion

The results presented here demonstrate that physical associations between distant chromosomal regions can occur with high frequency in interphase nuclei. These interactions are dramatically influenced by the developmental stage of the particular tissue and in some cases by temperature, and can result in perturbations of nuclear architecture that correlate with variegated gene expression. These results are consistent with the extensive homologous pairing observed between Drosophila polytene chromosomes, even in the presence of massive chromosome rearrangements. Here, we have finally extended this phenomenon to include diploid cells that, unlike polytene tissues, have not exited the mitotic cell cycle (Smith and Orr-Weaver, 1991). Moreover, our findings demonstrate a powerful impact of sequences other than centromeres and telomeres on the architecture of the interphase nucleus.

We have shown that the insertion of heterochromatin at the *bw* locus causes the gene to associate with centromeric heterochromatin during postembryonic development. We propose that this association is based on homology. The heterochromatic insertion in bw^D contains more than a megabase of AAGAG repeats (A. F. D. and J. W. S., unpublished data). This same simple repeated sequence also comprises over 5 Mb of the heterochromatin flanking the chromosome 2 centromere (Lohe et al., 1993). If either this sequence or proteins that bind to it can self-associate, this could result in the observed association between bw^D and the centromeric heterochromatin of chromosome 2.

We also report that the bw^D insertion targets the *bw* locus to the nuclear periphery. However, genetic results have demonstrated that the silencing effect of bw^D is influenced by its distance from centromeric heterochromatin (Talbert et al., 1994; Henikoff et al., 1995). Since nuclear envelope association of bw^D occurs in embryos, even when the insertion is physically isolated from centric heterochromatin, this strongly suggests that it is incidental to the mechanism of silencing and that it is physical interaction between bw^D and centric heterochromatin that mediates transcriptional repression.

Intrachromosomal Contacts Are Involved in Biological Phenomena in Many Organisms

The bw^D insertion affects the position of the *bw* gene specifically in relation to the pericentric AACAC satellite on chromosome 2, but not in relation to satellite DNA in general. We infer that the bw^D insertion interacts intrachromosomally with the centromeric heterochromatin of chromosome 2. Both cytological and molecular evidence suggest that the intrachromosomal association between bw^D and centromeric heterochromatin results from the normal arrangement of chromosomes in the interphase nucleus.

Cytological examination of mammalian interphase nuclei has shown that individual chromosomes tend to occupy exclusive territories, rather than intermingling extensively (reviewed by Haaf and Schmid, 1991). Direct evidence that chromosomes are restricted to subdomains in interphase Drosophila nuclei comes from at least three sources. First, examination of the arrangement of polytene nuclei has revealed that individual chromosome arms never intertwine (Mathog et al., 1984;

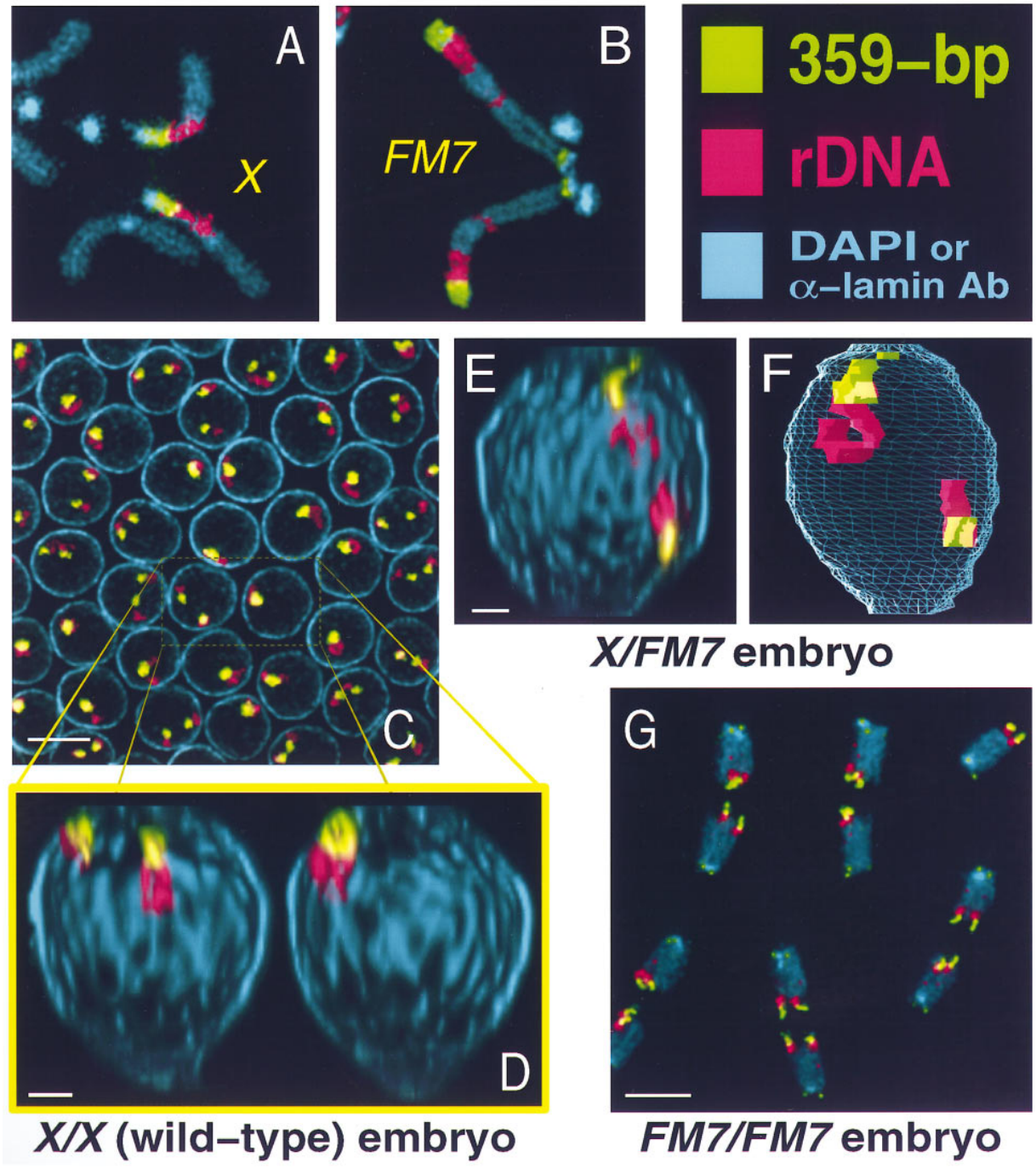

Figure 7. Nuclear Organization of Normal and Inverted X Chromosomes in Drosophila Embryos

(A) and (B) Mitotic chromosomes hybridized to indicate the positions of the 359 bp (green) and rDNA (magenta) repeats on X and FM7. On the normal X chromosome, these sequences both lie in the centric heterochromatin, but on FM7 most of the 359 bp repeats and all the rDNA are translocated to distal positions.

(C) and (D) The distribution of these sequences during interphase in female (X/X) wild-type embryos. In this embryo, fixed during the fourteenth interphase, some of the nuclei show pairing between homologous X chromosomes, but this pairing is not yet complete, as previously seen for the histone locus on chromosome 2 (Hiraoka et al., 1993). (D) is a lateral projection through the two adjacent nuclei enclosed by the small box in (C), in which the positions of the X heterochromatin along the apical–basal axis can be seen. The X heterochromatin localizes apically, as expected from its proximal position on the chromosome.

(E) and (F) show an interphase nucleus from a heterozygous X/FM7 embryo. The signals from the normal X are located apically, but the distal heterochromatin on FM7 localizes to the basal region. This physical separation prevents pairing between the two regions.

The interphase polarity observed in interphase nuclei in such embryos may result from frequent mitotic divisions, illustrated by the anaphase embryo shown in (G).

Scale bars in (D) and (E), 1 μm; scale bars in (C) and (G), 5 μm.

Hochstrasser et al., 1986). Second, prematurely condensed interphase chromosomes in Drosophila embryos deprived of oxygen remain well separated from one another (Foe and Alberts, 1985). Third, we have used probes to paint whole chromosomes in interphase nuclei from embryos and neuroblasts. In these preparations, individual chromosomes occupy distinct domains (A. F. D. and J. W. S., unpublished data), as seen in mammalian cells.

The proximity of particular loci during interphase has also been inferred from frequencies of somatic cell recombination or transposition. Exchange of DNA between two chromosomal positions implies that they are physically close together at the time this event occurs. In plants (Van Schaik and Brink, 1959), mammals (Hellgren, 1992; Godwin et al., 1994), and fungi (see below), ectopic recombination tends to occur intrachromosomally, and most often between sites that lie close together on the same chromosome. In Drosophila, strong preferences for intrachromosomal recombination have been demonstrated by irradiating embryos (Hilliker, 1985) and by excising transposable elements later in development (Blackman et al., 1987; Engels et al., 1994).

Studies in the budding yeast Saccharomyces cerevisiae demonstrate the same preference for intrachromosomal exchange. The mating type (**a** or α) of a yeast cell is determined by information encoded at the *MAT* locus on chromosome III. A cell can switch its mating type by activating the HO site-specific endonuclease, which makes a double-strand break at this locus, leading to transposition of a mating type allele from one of two silent donor loci located near each end of chromosome III at a distance of either 80 or 200 kb (Riles et al., 1993). If either the donor locus or the *MAT* locus is moved to a different chromosome, mating-type switching still occurs by the same mechanism, but the efficiency of repair following HO-induced cleavage drops dramatically (Rine and Herskowitz, 1980; Haber et al., 1981; Weiler and Broach, 1992). Furthermore, Lichten and Haber (1989) have shown that other types of mitotic intrachromosomal recombination between homologous sites up to a distance of 70 kb are preferred over interchromosomal recombination events.

The Persistence of Long-Distance Associations

While studies of mitotic recombination have correctly predicted the occurrence of physical interactions between distant chromosome regions, one issue that this experimental approach cannot address is the stability of such associations. We detected interaction between bw^D and centromeric heterochromatin in up to 86% of neuroblast nuclei examined. Since these measurements come from single time-points within asynchronous populations of nuclei, the associations must be sustained for a large portion of interphase. If such interactions were only fleeting, we might not have detected them at all using this cytological approach.

The Role of Heterochromatin in Long-Distance Chromosome Associations

Data from studies of mitotic recombination and other genetic phenomena demonstrate that regions outside the heterochromatin can physically associate in somatic cells. However, a variety of observations suggests that heterochromatin participates in such interactions with particularly high affinity. For example, ectopic fibers observed in Drosophila polytene nuclei frequently connect regions containing intercalary heterochromatin (Kauffman and Iddles, 1963), reflecting physical contact between such regions (Pardue, 1986).

This tendency of heterochromatin to participate in homologous associations is likely to be a consequence of its normal biological role in maintaining alignment between homologous chromosomes during mitosis and meiosis. When sister chromatids begin to separate at metaphase, persistent connections are detected cytologically between their heterochromatic regions (Carmena et al., 1993). Moreover, both genetic and cytological studies show that in Drosophila female meiosis, heterochromatin can maintain physical association between nonrecombinant homologous chromosomes and enable them to segregate from each other (Hawley et al., 1992; Dernburg et al., submitted; Karpen et al., submitted). In both of these examples, homologous heterochromatic pairing persists under conditions where euchromatic regions are separated. The basis for this "stickiness" of heterochromatin is still unknown, but one possibility is that the repeated nature of heterochromatic regions may provide a large number of binding sites for specific proteins. If such proteins can form multimeric complexes, this would provide a mechanism for specific physical contacts between homologous regions.

Why Is Centromeric Heterochromatin Special?

In conjunction with genetic evidence, our results indicate that the bw^D heterochromatic insertion represses *bw* expression in heterozygotes by mediating physical contact of the intact *bw* copy with centromeric heterochromatin. Like other examples of PEV, the variegation of *bw* caused by bw^D is apparently caused by physical contact with centromeric heterochromatin, but in this case the association results from long-distance looping rather than linear proximity along the chromosome. Surprisingly, pairing of $bw+$ with bw^D does not seem to be sufficient to silence the normal copy of the gene, despite the presence of over 1 Mb of centromeric satellite sequences within the bw^D insertion. This implies that there is something inherently different between centromeric heterochromatin and heterochromatin located elsewhere on the chromosome, even if its sequence composition is identical.

This difference is unlikely to be due to a mass effect, since genes will variegate if located near heterochromatin on a minichromosome that in its entirety is smaller than the bw^D insertion (Karpen and Spradling, 1990). The data presented here also suggest that the difference cannot be due to localization of centromeric heterochromatin to a particular region of the nucleus, since we have shown that the centromeric regions of different chromosomes are widely dispersed in interphase cells from imaginal disks and neuroblasts. Nor is it likely that the determining factor is nuclear envelope association, since we have observed association of the bw^D insertion

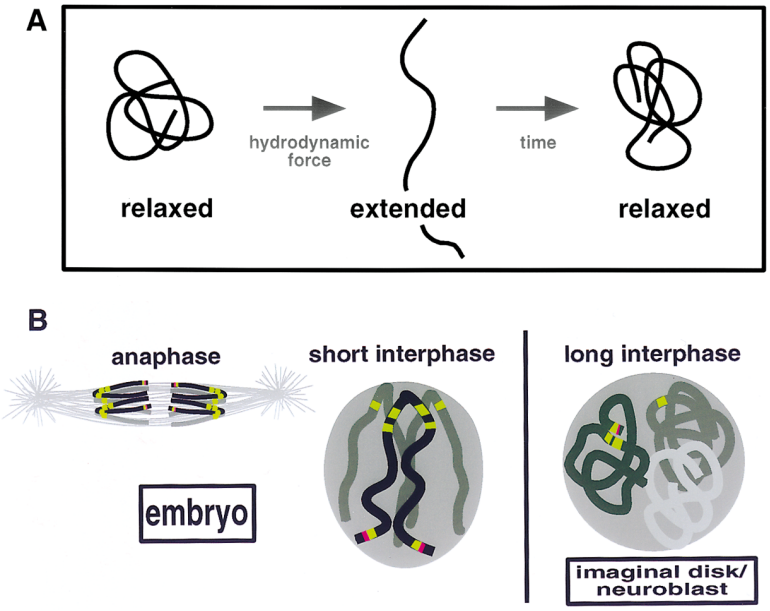

Figure 8. A Polymer Diffusion Model for Interphase Chromosome Organization

(A) The behavior of an elastic polymer in solution (adapted from Freifelder, 1976). Entropy drives a long polymer into a compact conformation in the absence of externally applied force. If the polymer is subjected to shear or hydrodynamic force, it will become extended. Once the force is removed, the polymer chain will return to a more favorable compact conformation.

(B) The behavior of interphase chromosomes may reflect these simple principles. In Drosophila embryos, mitotic division is extremely frequent, and during the short intervening interphases, chromosomes have little time to relax from the Rabl conformation induced by their anaphase movement. Thus, centromeric blocks of the AAGAG satellite (green) never come into contact with distal genes such as *bw* (magenta). However, in later stages of development when interphase is much longer, we detect physical association between centromeric heterochromatin and the *bw* gene located distally on the same chromosome. Intrachromosomal contacts are favored, because individual chromosomes occupy distinct domains within the nucleus.

with the nuclear envelope in embryos, where it is isolated from centric heterochromatin.

We are left with the possibility that the transcriptional effects of centric heterochromatin are due to physical linkage with the centromere itself. Since the centromere possesses a unique ability to form a kinetochore, it follows that there are cellular proteins that recognize the centromere and no other site on the chromosome. Perhaps there are consequences of proximity to this region that are only manifested through a "spreading" mechanism along the chromosome.

A Model for Intrachromosomal Interaction Based on Random–Walk Polymer Behavior

We have observed major differences in nuclear organization between embryonic nuclei and those from larval stages. To some extent, these changes may be mediated by developmentally regulated patterns of gene expression. However, they may also reflect the effects of basic thermodynamic principles that operate on all long polymers (Figure 8).

Evidence from FISH analysis of interphase nuclei suggests that on a megabase scale, the organization of entire chromosomes is accurately approximated by mathematical models of random–walk polymers (Sachs et al., 1995; Yokota et al., 1995). Such long-chain polymers are entropically driven towards compact conformations (Freifelder, 1976; Bustamante et al., 1994), unlike the extended and highly nonrandom Rabl conformation that we have characterized in embryonic nuclei from Drosophila (after Carl Rabl, who first described such chromosome polarity in amphibian nuclei in 1885). We propose that the extended conformation observed in blastoderm embryos simply reflects the fact that the chromosomes are frequently subjected to hydrodynamic forces as they undergo mitotic division every 10–20 min (Foe and Alberts, 1983; Figure 7G).

By the second and third instar larval stages, interphase in imaginal tissues has been estimated to span several hours (Graves and Schubiger, 1982). At these stages, there is a high frequency of interaction between regions far apart on chromosome 2 (Table 1). We propose that random–walk diffusion of the chromosome occasionally brings bw^D into proximity with homologous centromeric heterochromatin, and this results in stable bonds that hold these regions apposed until the next mitosis. This model is consistent with genetic data showing the dependence of transcriptional silencing by bw^D on its distance from centromeric heterochromatin (Talbert et al., 1994; Henikoff et al., 1995), since for a flexible polymer the frequency at which two points will come into contact is inversely proportional to the distance between them along the polymer chain. (More precisely, for a random–walk polymer this frequency is inversely proportional to $N^{3/2}$, where N is the number of theoretical links separating two points in the chain; Doi and Edwards, 1986).

From existing data, we cannot rule out the possibility that contact between bw^D and centric heterochromatin results from an active process that brings homologous regions together from a great distance. However, this passive diffusion model can also help to explain why the *trans*-inactivation of *bw* expression by bw^D is so strong. Heterozygous $bw^D/+$ flies produce only 2% of wild-type pteridine pigment levels (Henikoff et al., 1995). Based on this model, we would expect to see an increase in long-distance associations during stages of development when mitotic division is less frequent, since under those conditions interphase chromosomes have even longer to diffuse within the nucleus. By the late pupal period, when *bw* is likely to be expressed in eye disks, they have completed their proliferation (reviewed by Wolff and Ready, 1993), and the frequency of association of bw^D with centromeric heterochromatin

would thus be expected to be even greater than that observed in larval nuclei.

Experimental Procedures

Fly Stocks

All wild-type flies were from an Oregon-R stock maintained at UCSF. A *bw*^{D} stock was furnished by S. Henikoff, and flies carrying the FM7a chromosome (Merriam, 1968; Lindsley and Zimm, 1992) were provided by R. S. Hawley. Unless otherwise specified, flies were raised at room temperature in bottles containing a yeast/glucose-rich medium.

Probes for In Situ Hybridization

Two different probes to the *bw* locus were used. A plasmid containing an 8.4 kb insert from the *bw* coding region (a gift of S. Henikoff) was used to mark the *bw* locus in embryonic nuclei. A P1 clone (Hartl et al., 1994) from the same region (DS03480) was provided by the Berkeley Drosophila Genome Project. Its origin from a single genomic site at cytological position 59E1–2 was confirmed by hybridization to polytene chromosomes. This probe was used to mark the *bw* locus in squash preparations.

The 359-bp repeat was synthesized by genomic PCR using primers designed from the published sequence (Hsieh and Brutlag, 1979). The AACAC, AAGAG, and dodeca satellite probes were all synthetic single-stranded oligonucleotides 35–46 bases in length. The rDNA probe comprised two plasmids with inserts spanning the 18S, 28S, and ITS regions (McKee and Karpen, 1990). Probes were enzymatically fragmented (except for the oligos) and 3′ end-labeled as described by Dernburg et al. (1996). Probes were fluorescently labeled with FluoroRed (Amersham) or hapten-labeled with digoxigenin–dUTP (Boehringer Mannheim) or biotin–dCTP (GIBCO BRL) and detected with fluorescent antibodies or avidin, respectively.

In Situ Hybridization

Eye/antennal disk and larval brain spreads were prepared by dissecting the appropriate tissue in Robb's saline (Ashburner, 1989), incubating for 10 min in 0.7% Na citrate and squashing in 45% acetic acid under a siliconized coverslip. Hybridization was carried out as described by Pardue (1986).

Embryos were fixed and hybridized using the procedure described by Dernburg et al. (1996). Following hybridization, they were stained with a monoclonal anti-lamin antibody (Fuchs et al., 1983) to mark the nuclear envelope. This was detected using a Cy5-conjugated goat anti-mouse 2° antibody (Jackson ImmunoResearch). In some cases, a hybridization probe was also detected with Cy5 but could be clearly segmented from the lamin signal based on intensity.

Whole-mount eye imaginal disks were dissected, fixed, and hybridized essentially as described for Drosophila spermatids by Dernburg et al. (1996), except that 0.1% deoxycholate and 0.1% Triton X-100 were included in the dissection buffer.

Microscopy and Image Analysis

All images were recorded with a scientific-grade cooled CCD camera (Photometrics, Tucson, AZ), using a wide-field fluorescence microscope system described in detail elsewhere (Hiraoka et al., 1990b). For three-dimensional specimens, data was collected by moving the sample through the focal plane of the lens at precise 0.25 μm increments. At each focal plane, images were recorded separately for each wavelength. Data stacks were then deconvolved with an empirical point-spread function using a constrained iterative method (Agard et al., 1989). Squash preparations were recorded as separate images for each wavelength at a single focal plane and then deconvolved with a two-dimensional point-spread function.

Measurements from the data were performed using IVE software (Chen et al., 1996). Distances in squash preparations were determined by marking each hybridization signal in a nucleus using a mouse and applying a local maximum-intensity search to attain accuracy and to avoid biasing the results. The circumference of each nucleus was traced from the DAPI fluorescence image. The area enclosed by the resulting polygon was recorded and from these values a diameter was calculated as $2 \times \sqrt{\text{area}/\pi}$. Nuclei that overlapped or deviated markedly from a circular shape were excluded from the analysis. To compensate for differences in nuclear size, which were presumed to result at least partly from differences between individual preparations, the measurements were normalized by dividing each distance value by the corresponding nuclear diameter. Typically 80–180 nuclei were recorded per field; at least four fields from separate specimens were analyzed for each sample. Histogram and scatter plots were generated using S-PLUS (MathSoft, Incorporated, Seattle, WA).

The representations of three-dimensional nuclei presented here are of two types: projections through stacks of intensity data, generated by either a maximum-intensity algorithm or using volume rendering (Dreibin et al., 1986); and wire frame/solid models constructed from the original data. All were pseudocolored to allow overlay of images recorded at different wavelengths.

Statistical Method for the Analysis of Mixture Distributions

Frequencies of nuclei exhibiting association were estimated as follows. We assume that in nuclei in which the *bw* locus does not associate with the AACAC satellite, the normalized *bw*–AACAC distances follow a normal distribution with parameters μ_1 and σ_1, truncated at 0 and 1, so that the density is

$$f_W(x) = \phi\left(\frac{x-\mu_1}{\sigma_1}\right) \Big/ \int_0^1 \phi\left(\frac{t-\mu_1}{\sigma_1}\right) dt,$$

where Φ is the density for a standard normal distribution. In nuclei in which the *bw* locus does associate with the AACAC satellite, the *bw*–AACAC distances are assumed to follow the same type of distribution, but with different parameters, μ_2 and σ_2, so that the density is

$$f_A(x) = \phi\left(\frac{x-\mu_2}{\sigma_2}\right) \Big/ \int_0^1 \phi\left(\frac{t-\mu_2}{\sigma_2}\right) dt.$$

Let $x_1,\ldots,x_n$ denote the normalized *bw*–AACAC distances for the wild-type cells, and let $y_1,\ldots,y_m$ denote the *bw*–AACAC distances for the *bw*^{D} cells. We assume that the x_i and y_i are independent. Moreover, the x_i are assumed to follow the distribution, f_W, whereas the y_i are considered to follow a mixture of f_W and f_A, so that their density is $pF_A(x) + (1-p)f_W(x)$. The mixing proportion, p, represents the frequency of *bw*^{D} nuclei exhibiting association.

We estimate the five parameters, μ_1, σ_1, μ_2, σ_2, and p, by maximum likelihood. Namely, we form the log likelihood

$$l(\mu_1, \sigma_1, \mu_2, \sigma_2, p) = \sum_{i=1}^{n} \log f_W(x_i) + \sum_{i=1}^{m} \log[pf_A(y_i) + (1-p)f_W(y_i)]$$

and choose as estimates the values that maximize this function. Standard deviations for our estimates were estimated using the bootstrap (Efron and Tibshirani, 1993). Calculations were performed using S-PLUS.

Acknowledgments

Analysis and display of our images were made possible through the tremendous efforts of Hans Chen, Paul Chan, and Diana Hughes. Advice on statistical analysis from Terry Speed, Peter Bacchetti, and Ray Sachs was very much appreciated. We thank Jeremy Minshull, Jeff Sekelsky, Scott Hawley, Elizabeth Blackburn, and Jim Haber for critical reading of the manuscript. This work was supported by the Howard Hughes Medical Institute Predoctoral Fellowships to A. F. D. and W. F. M. and by a National Institutes of Health grant to J. W. S.

Received March 13, 1996; revised April 12, 1996.

References

Abad, J.P., Carmena, M., Baars, S., Saunders, R.D., Glover, D.M., Ludena, P., Sentis, C., Tyler, S.C., and Villasante, A. (1992). Dodeca

satellite: a conserved G+C-rich satellite from the centromeric heterochromatin of Drosophila melanogaster. Proc. Natl. Acad. Sci. USA *89*, 4663–4667.

Agard, D.A., Hiraoka, Y., Shaw, P., and Sedat, J.W. (1989). Fluorescence microscopy in three dimensions. Meth. Cell Biol. *30*, 353–377.

Ashburner, M. (1989). Drosophila: A Laboratory Manual. (Cold Spring Harbor, New York: Cold Spring Harbor Laboratory Press).

Blackman, R.K., Grimaila, R., Koehler, M.M., Gelbart, W.M. (1987). Mobilization of hobo elements residing within the decapentaplegic gene complex: suggestion of a new hybrid dysgenesis system in Drosophila melanogaster. Cell *49*, 497–505.

Bustamante, C., Marko, J.F., Siggia, E.D., and Smith, S. (1994). Entropic elasticity of lambda-phage DNA [letter]. Science *265*, 1599–1600.

Carmena, M., Abad, J.P., Villasante, A., and Gonzalez, C. (1993). The Drosophila melanogaster dodeca satellite sequence is closely linked to the centromere and can form connections between sister chromatids during mitosis. J. Cell Sci. *105*, 41–50.

Chen, H., Hughes, D.D., Chan, T.-A., Sedat, J.W., and Agard, D.A. (1996). IVE (image visualization environment): a software platform for all three-dimensional microscopy applications. J. Struct. Biol. *116*, 56–60.

Cremer, T., Kurz, A., Zirbel, R., Dietzel, S., Rinke, B., Schrock, E., Speicher, M.R., Mathieu, U., Jauch, A., Emmerich, P., Schertan, H., Ried, T., Cremer, C., Lichter, P. (1993). Role of chromosome territories in the functional compartmentalization of the cell nucleus. Cold Spring Harbor Symp. Quant. Biol. *58*, 777–792.

Dernburg, A.F., Daily, D., Yook, K.J., Corbin, J.A., Sedat, J.W., and Sullivan, W. (1996). Selective loss of compound-chromosome bearing sperm in the Drosophila female. Genetics *143*, in press.

Doi, M., and Edwards, S.F. (1986). The Theory of Polymer Dynamics. (Oxford: Clarendon Press).

Dreesen, T.D., Johnson, D.H., and Henikoff, S. (1988). The brown protein of Drosophila melanogaster is similar to the white protein and to components of active transport complexes. Mol. Cell. Biol. *8*, 5206–5215.

Dreesen, T.D., Henikoff, S., and Loughney, K. (1991). A pairing-sensitive element that mediates *trans*-inactivation is associated with the Drosophila *brown* gene. Genes Dev. *5*, 331–340.

Dreibin, R.A., Carpenter, L., and Hanranhan, P. (1986). Volume rendering. Comput. Graph. *22*, 65–75.

Efron, B., and Tibshirani, R.J. (1993). An Introduction to the Bootstrap (New York: Chapman and Hall).

Engels, W.R., Preston, C.R., Johnson-Schlitz, D.M. (1994). Long-range *cis* preference in DNA homology search over the length of a Drosophila chromosome. Science *263*, 1623–1625.

Foe, V.E., and Alberts, B.M. (1983). Studies of nuclear and cytoplasmic behaviour during the five mitotic cycles that precede gastrulation in Drosophila embryogenesis. J. Cell Sci. *61*, 31–70.

Foe, V.E., and Alberts, B.M. (1985). Reversible chromosome condensation induced in Drosophila embryos by anoxia: visualization of interphase nuclear organization. J. Cell Biol. *100*, 1623–1636.

Freifelder, D. (1976). Physical Biochemistry (San Francisco: W.H. Freeman and Company).

Fuchs, J.P., Giloh, H., Kuo, C.H., Saumweber, H., and Sedat, J. (1983). Nuclear structure: determination of the fate of the nuclear envelope in Drosophila during mitosis using monoclonal antibodies. J. Cell Sci. *64*, 331–349.

Godwin, A.R., Bollag, R.J., Christie, D.M., and Liskay, R.M. (1994). Spontaneous and restriction enzyme–induced chromosomal recombination in mammalian cells. Proc. Natl. Acad. Sci. USA *91*, 12554–12558.

Graves, B.J., and Schubiger, G. (1982). Cell cycle changes during growth and differentiation of imaginal leg discs in Drosophila melanogaster. Dev. Biol. *93*, 104–110.

Haaf, T., and Schmid, M. (1991). Chromosome topology in mammalian interphase nuclei. Exp. Cell Res. *192*, 325–332.

Haber, J.E., Rowe, L., and Rogers, D.T. (1981). Transposition of yeast mating type genes from two translocations of the left arm of chromosome III. Mol. Cell. Biol. *1*, 1106–1119.

Hartl, D.L., Nurminsky, D.I., Jones, R.W., and Lozovskaya, E.R. (1994). Genome structure and evolution in Drosophila: applications of the framework P1 map. Proc. Natl. Acad. Sci. USA *91*, 6824–6829.

Hawley, R.S., Irick, H., Zitron, A.E., Haddox, D.A., Lohe, A., New, C., Whitley, M.D., Arbel, T., Jang, J., McKim, K., and Childs, G. (1992). There are two mechanisms of achiasmate segregation in Drosophila females, one of which requires heterochromatic homology. Dev. Genet. *13*, 440–467.

Hellgren, D. (1992). Mutagen-induced recombination in mammalian cells in vitro. Mutat. Res. *284*, 37–51.

Henikoff, S. (1994). A reconsideration of the mechanism of position effect. Genetics *138*, 1–5.

Henikoff, S. (1996). A pairing-looping model for position–effect variegation in Drosophila. In Genomes: Proceedings of the 21st Stadler Genetics Symposium, J.P. Gustafson and R.B. Flavell, eds. (New York: Plenum Press), in press.

Henikoff, S., Jackson, J.M., and Talbert, P.B. (1995). Distance and pairing effects on the *brown*^{Dominant} heterochromatic element in Drosophila. Genetics *140*, 1007–1017.

Hilliker, A.J. (1985). Assaying chromosome rearrangement in embryonic interphase nuclei of *Drosophila melanogaster* by radiation-induced interchanges. Genet. Res. *47*, 13–18.

Hiraoka, Y., Agard, D.A., and Sedat, J.W. (1990a). Temporal and spatial coordination of chromosome movement, spindle formation, and nuclear envelope breakdown during prometaphase in *Drosophila melanogaster* embryos. J. Cell Biol. *111*, 2815–2828.

Hiraoka, Y., Sedat, J.W., and Agard, D.A. (1990b). Determination of three-dimensional imaging properties of a light microscope system: partial confocal behavior in epifluorescence microscopy. Biophys. J. *57*, 325–333.

Hiraoka, Y., Dernburg, A.F., Parmelee, S.J., Rykowski, M.C., Agard, D.A., and Sedat, J.W. (1993). The onset of homologous chromosome pairing during *Drosophila melanogaster* embryogenesis. J. Cell Biol. *120*, 591–600.

Hochstrasser, M., Mathog, D., Gruenbaum, Y., Saumweber, H., and Sedat, J.W. (1986). Spatial organization of chromosomes in the salivary gland nuclei of Drosophila melanogaster. J. Cell Biol. *102*, 112–123.

Hsieh, T., and Brutlag, D. (1979). Sequence and sequence variation within the 1.688 g/cm3 satellite DNA of *Drosophila melanogaster*. J. Mol. Biol. *135*, 465–481.

Karpen, G.H., and Spradling, A.C. (1990). Reduced DNA polytenization of a minichromosome region undergoing position–effect variegation in Drosophila. Cell *63*, 97–107.

Kauffman, B.P., and Iddles, M.K. (1963). Ectopic pairing in salivary gland chromosomes of *Drosophila melanogaster* I: distribution patterns in relation to puffing. Acta. Biol. Port. *7*, 225–248.

Lichten, M., and Haber, J.E. (1989). Position effects in ectopic and allelic mitotic recombination in *Saccharomyces cerevisiae*. Genetics *123*, 261–268.

Lindsley, D.L., and Zimm, G.G. (1992). The Genome of *Drosophila melanogaster* (San Diego: Academic Press).

Lohe, A.R., Hilliker, A.J., and Roberts, P.A. (1993). Mapping simple repeated DNA sequences in heterochromatin of Drosophila melanogaster. Genetics *134*, 1149–1174.

Makunin, I.V., Pokholkova, G.V., Zakharkin, S.O., Kholodilov, N.G., and Zhimulev, I.F. (1995). Isolation and characterization of the repeated DNA sequences from the centromeric heteochromatin of the second chromosome of *Drosophila melanogaster*. Doklady Academii Nauk (Reports of the Russian Academy of Sciences, in Russian) *344*, 266–269.

Manuelidis, L. (1990). A view of interphase chromosomes. Science *250*, 1533–1540.

Marshall, W.F., Dernburg, A.F., Harmon, B., Agard, D.A., and Sedat,

J.W. (1996). Specific interactions of chromatin with the nuclear envelope: positional determination within the nucleus in D. melanogaster. Mol. Cell. Biol. *7*, in press.

Mathog, D., Hochstrasser, M., Gruenbaum, Y., Saumweber, H., and Sedat, J. (1984). Characteristic folding pattern of polytene chromosomes in Drosophila salivary gland nuclei. Nature *308*, 414–421.

McKee, B.D., and Karpen, G.H. (1990). Drosophila ribosomal RNA genes function as an X–Y pairing site during male meiosis. Cell *61*, 61–72.

Merriam, J.R. (1968). FM7: first multiple seven. DIS *43*, 64.

Palladino, F., and Gasser, S.M. (1994). Telomere maintenance and gene repression: a common end? Curr. Opin. Cell Biol. *6*, 373–379.

Pardue, M.L. (1986). In situ hybridization to DNA of chromosomes and nuclei. In Drosophila: A Practical Approach, D.B. Roberts, ed. (Oxford: IRL Press, Limited), pp. 111–137.

Riles, L., Dutchik, J.E., Baktha, A., McCauley, B.K., Thayer, E.C., Leckie, M.P., Braden, V.V., Depke, J.E., and Olson, M.V. (1993). Physical maps of the six smallest chromosomes of *Saccharomyces cerevisiae* at a resolution of 2.6 kilobase pairs. Genetics *134*, 81–150.

Rine, J., and Herskowitz, I. (1980). The *trans* action of HMRa in mating type interconversion. Mol. Gen. Genet. *180*, 99–105.

Sachs, R.K., van den Engh, G., Trask, B., Yokota, H., and Hearst, J.E. (1995). A random–walk/giant-loop model for interphase chromosomes. Proc. Natl. Acad. Sci. USA *92*, 2710–2714.

Slatis, H.M. (1955). A reconsideration of the *brown-dominant* position effect. Genetics *40*, 246–251.

Smith, A.V., and Orr-Weaver, T.L. (1991). The regulation of the cell cycle during Drosophila embryogenesis: the transition to polyteny. Development *112*, 997–1008.

Spofford, J. (1976). Position–effect variegation. In The Genetics and Biology of Drosophila, volume 1c, M. Ashburner and E. Novitski, eds. (London; New York: Academic Press), pp. 955–1018.

Talbert, P.B., LeCiel, C.D., and Henikoff, S. (1994). Modification of the Drosophila heterochromatic mutation *brown*^{Dominant} by linkage alterations. Genetics *136*, 559–571.

Tartof, K.D., and Henikoff, S. (1991). *Trans*-sensing effects from Drosophila to humans. Cell *65*, 201–203.

Titterington, D.M., Smith, A.F.M., and Makov, U.E. (1985). Statistical Analysis of Finite Mixture Distributions (New York: Wiley).

Van Schaik, N.W., and Brink, R.A. (1959). Transpositions of *Modulator*, a component of the variegated pericarp allele in maize. Genetics *44*, 725–738.

Weiler, K.S., and Broach, J.R. (1992). Donor locus selection during *Saccharomyces cerevisiae* mating type interconversion responds to distant regulatory signals. Genetics *132*, 929–942.

Weiler, K.S., and Wakimoto, B.T. (1995). Heterochromatin and gene expression in Drosophila. Annu. Rev. Genet. *29*, 577–605.

Wolff, T., and Ready, D.F. (1993). Pattern formation in the Drosophila retina. In The Development of *Drosophila melanogaster*, M. Bate and A. Martinez Arias, eds. (Plainview, New York: Cold Spring Harbor Laboratory Press), pp. 1277–1325.

Yokota, H., van den Engh, G., Hearst, J.E., Sachs, R.K., and Trask, B.J. (1995). Evidence for the organization of chromatin in megabase pair–sized loops arranged along a random walk path in the human G0/G1 interphase nucleus. J. Cell Biol. *130*, 1239–1249.

Note Added in Proof

The paper referred to as Dernburg et al., submitted is now in press: Dernburg, A.F., Sedat, J.W., and Hawley, R.S. (1996). Direct evidence of a role for heterochromatin in meiotic chromosome segregation. Cell *85*, in press.